

REPORT DOCUMENTATION PAGEForm Approved
OMB No. 0704-0188


Public reporting burden for this collection of information is estimated to average 1 hour per response, including the time for reviewing instructions, searching existing data sources, gathering and maintaining the data needed, and completing and reviewing this collection of information. Send comments regarding this burden estimate or any other aspect of this collection of information, including suggestions for reducing this burden to Department of Defense, Washington Headquarters Services, Directorate for Information Operations and Reports (0704-0188), 1215 Jefferson Davis Highway, Suite 1204, Arlington, VA 22202-4302. Respondents should be aware that notwithstanding any other provision of law, no person shall be subject to any penalty for failing to comply with a collection of information if it does not display a currently valid OMB control number. PLEASE DO NOT RETURN YOUR FORM TO THE ABOVE ADDRESS.

1. REPORT DATE (DD-MM-YYYY) 02-28-2003		2. REPORT TYPE Technical Abstract		3. DATES COVERED (From - To)	
4. TITLE AND SUBTITLE Equilibrium and Non-Equilibrium Effects in Pitch Wetting				5a. CONTRACT NUMBER	
				5b. GRANT NUMBER	
				5c. PROGRAM ELEMENT NUMBER	
6. AUTHOR(S) P.G. Wapner, W.P. Hoffman, Robert Hurt, Gernot Krammer				5d. PROJECT NUMBER 2306	
				5e. TASK NUMBER M1B3	
				5f. WORK UNIT NUMBER	
7. PERFORMING ORGANIZATION NAME(S) AND ADDRESS(ES) ERC, Inc. 10 E. Saturn Blvd. Edwards AFB, CA 93524-7680				8. PERFORMING ORGANIZATION REPORT NUMBER AFRL-PR-ED-AB-2003-050	
9. SPONSORING / MONITORING AGENCY NAME(S) AND ADDRESS(ES) Air Force Research Laboratory (AFMC) AFRL/PRS 5 Pollux Drive Edwards AFB CA 93524-7048				10. SPONSOR/MONITOR'S ACRONYM(S)	
				11. SPONSOR/MONITOR'S NUMBER(S) AFRL-PR-ED-AB-2003-050	
12. DISTRIBUTION / AVAILABILITY STATEMENT Approved for public release; distribution unlimited.					
13. SUPPLEMENTARY NOTES					
14. ABSTRACT <div style="text-align: right; padding-right: 50px;">BEST AVAILABLE COPY 20031003 097</div>					
15. SUBJECT TERMS					
16. SECURITY CLASSIFICATION OF:			17. LIMITATION OF ABSTRACT	18. NUMBER OF PAGES	19a. NAME OF RESPONSIBLE PERSON
					Sheila Benner
a. REPORT Unclassified	b. ABSTRACT Unclassified	c. THIS PAGE Unclassified	A		19b. TELEPHONE NUMBER (include area code) (661) 275-5963

Standard Form 298 (Rev. 8-98)
Prescribed by ANSI Std. Z39.18

FILE

MEMORANDUM FOR PRS (In-House/Contractor Publication)

FROM: PROI (STINFO) 

28 Feb 2003

SUBJECT: Authorization for Release of Technical Information, Control Number: **AFRL-PR-ED-AB-2003-050**
P.G. Wapner (ERC); W.P. Hoffman (AFRL/PRSM); Robert Hurt; Gernot Krammer, "Equilibrium and
Non-Equilibrium Effects in Pitch Wetting"

Carbon 2003 Conference
(Oviedo, Spain, 6-10 July 2003) (Deadline: 30 Mar 2003)

(Statement A)

BEST AVAILABLE COPY

Equilibrium and Non-Equilibrium Effects in Pitch Wetting

P.G. Wapner[†], R.H. Hurt^{††}, Gernot Krammer^{†††}, W.P. Hoffman^{††††}

[†]ERC Inc., Edwards, CA, 93524 USA, ^{††}Brown University, Providence, Rhode Island, 02912 USA,

^{†††}Technical University of Graz, Graz, Austria, ^{††††}Air Force Research Laboratory, Edwards, CA, 93524 USA

Abstract

The wetting behavior of pitch plays an important role in impregnation processes for densification, in deposition within processing equipment for heavy hydrocarbons, and in the synthesis of new pitch-based templated carbon forms. This paper reports on an experimental and theoretical study of the fundamental wetting behavior of mesophase pitch on well-characterized flat substrates. Contact angle measurements are reported as a function of temperature, time, and substrate chemistry. There is strong evidence that pitch wetting is determined both by equilibrium effects (liquid surface tension, solid surface energy and their dispersive and polar components) and by non-equilibrium effects (spreading kinetics). In the high temperature regime the surface energies of the pitch and substrate are the most important factors determining wetting behavior, while pitch viscosity plays a dominant role in the lower temperature regime where spontaneous droplet spreading rates can be extremely slow.

Keywords: A. pitch, mesophase, B. impregnation, C. modeling, D. viscoelasticity

1. INTRODUCTION

The wetting behavior of pitch plays an important role in the impregnation process for composites [1], in deposition and fouling within processing equipment for heavy hydrocarbons, and in the synthesis of new carbon forms derived from the infiltration of pitch into porous templates [2]. While there have been many studies of pitch rheology, especially under conditions relevant to fiber spinning [3], there have been few systematic studies of the true wetting behavior of pitch [4] or mesophase pitch [5]. Here we report on a fundamental study of pitch wetting on well-characterized flat substrates as a first step toward the understanding of fiber wetting. Experimental measurements are made of pitch/substrate contact angle as a function of temperature, surface properties, and time, and the results are compared to equilibrium and dynamic theories of wetting and spreading.

2. EXPERIMENTAL

This set of experiments used the naphthalene-derived AR mesophase (HP grade) supplied courtesy of Mitsubishi Gas Chemical. The mesophase was first dried under vacuum for 24 hours at 125 °C in the as-received form (small rod-shaped drops weighing 25 milligrams on average). It was then cooled to ambient temperature and three grams were loaded into a small tube-shaped stainless steel reservoir equipped at the bottom with a 0.025-inch in diameter flat-tipped syringe needle. The reservoir was then positioned in a insulated cylindrical vertical oven 1 1/2-inches in diameter by 6-inches tall. The oven is equipped with triple-pane pyrex windows front and rear to allow continuous back illumination and viewing of AR mesophase drops as they are placed on a given substrate. An elevator-type mechanism allows 1-inch in diameter by 3-inch in length pyrex test tubes to be raised up into the oven directly beneath the syringe needle. A 1/16-inch in diameter metal tube placed along

side the stainless steel reservoir directs a nitrogen gas flow into the periphery of the test tube at a rate of 100 cc/minute. This is done to purge any oxygen from the system. The purge tube is wrapped around the reservoir to let temperature equilibrium be established with the rest of the system. The reservoir is also shaped so that it sits directly on the test tubes, but allows enough leakage for nitrogen purge gas to escape. Substrates are placed on a lightweight aluminum sample holder that fits snugly inside the test tubes. Purge gas can easily sweep around and underneath the substrate, once it is introduced into the oven. An experiment is initiated by setting the oven temperature controller set point to a desired temperature and positioning a test tube (without a substrate) underneath it. Thermocouples in the oven, reservoir, and resting on the empty sample holder, monitor temperatures at these locations. Within 10 minutes, the oven temperature is reached and starts cycling plus/minus 2 °C. The reservoir and sample holder reach equilibrium temperatures within about 10 additional minutes. They both are normally about 10 °C cooler than the oven itself due to heat flux outwards. A slight inert gas pressure is then applied to the reservoir to expel AR mesophase from the syringe needle. The test tube is then lowered and replaced with a new one equipped with a sample holder containing a freshly-cleaved sample of HOPG. The HOPG typically measures 1-cm by 1-cm by 2-mm. Temperatures are again allowed to equilibrate, which takes roughly 10 minutes. A drop of AR mesophase is formed by pressurization and then allowed to fall onto the substrate. Its spreading is observed with an InfiniVar[™] continuously-focusable microscope from Edwards Scientific, Inc. that is equipped with a high-resolution CCD video camera which feeds a video signal at 30 frames/second to an FTA 100 Drop Shape Analyzer. The FTA 100 is manufactured by First Ten Angstroms, Inc., of Portsmouth, VA and its software reduces the data to actual contact angles. The temperature of the measurement is considered to be the average of the

reservoir and sample holder temperatures. These are typically within several degrees of one another.

Additional measurements were made on a series of substrates at a single temperature at Kruss USA in order to understand the nature of pitch/substrate energetic interactions. The temperature of 325 °C was chosen to be high enough to provide sufficient fluidity to reach the equilibrium or near-equilibrium state yet low enough to minimize bubble formation and swelling. The surfaces were characterized first for their dispersive and polar surface energy components using the Owens-Wendt theory [6] applied to contact angle measurements involving standard liquids of differing polarity.

3. RESULTS AND DISCUSSION

The experimental results are given in Figs. 1 and 2 and Tables 1 and 2. The early measurements in Fig. 1 showed very high contact angles at temperature below about 280 °C with sharp decreases to nearly complete wetting above 300 °C. This behavior is not typical of other liquids, which most often show only modest and gradual increases in contact angle with decreasing temperature [7].

These early experiments also showed poor reproducibility, which was found to be due to the presence of an oxidized skin on the AR pellets. Further experiments used crushed and preheated (pre-softened) droplets to avoid the skin effect. The later experiments were also specifically designed to explicitly measure the time-dependence of contact angles, which is key to understanding the behavior at all but the highest temperatures studied.

Figure 2 shows results of the dynamic contact angle measurements on freshly cleaved HOPG basal planes. Spreading times are strongly temperature dependent, varying from about 1 second at 371 °C to well over 100 sec at 325 °C. Equilibrium wetting experiments begin to be impractical at temperature below 325 °C.

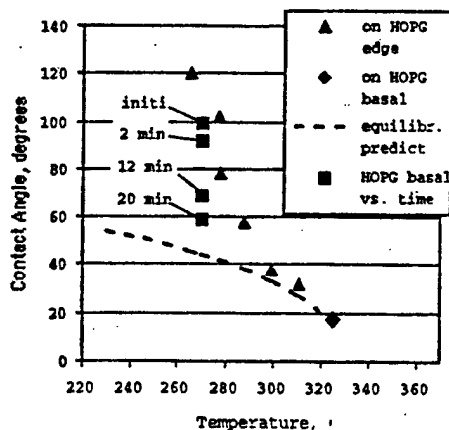


Figure 1. Early measurements of contact angle as a function of temperature for AR mesophase on HOPG. The dashed line shows the expected behavior from equilibrium theories starting from the 325 °C data point (assumed to be near equilibrium) and using a typical

value for the temperature coefficient of liquid surface tension, $\gamma/dT = -0.15 \text{ mJ/m}^2\text{-K}$. (For example, $\gamma/dT = -0.133$ for benzene, -0.102 for phenol, and -0.088 for glycerol). The data at temperatures below about 300 °C show much higher contact angles and a time-dependence that indicate non-equilibrium states.

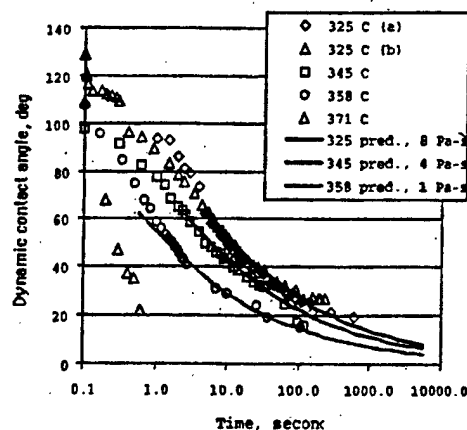


Figure 2. Dynamic contact angles for AR mesophase on freshly cleaved HOPG basal plane using the preheated droplet technique: Symbols: experimental measurements, Lines: dynamic spreading theory predictions for viscosities given in legend. Note that the dynamic spreading theories are applicable only to low contact angles ($< 60^\circ$).

Tables 1 and 2 give the measurements of pitch surface tension by the pendent droplet technique and equilibrium or near-equilibrium contact angles on a variety of solid surfaces. Contact angle is seen to depend strongly on the nature of the surface ranging from 23° on glassy carbon to 66.5° on PTFE. For many materials (glasses, ceramics, metals) the angles lie between 20° and 40°. A criterion for successful wetting is often defined as $\theta < 90^\circ$, in which case it can be said that pitch wets all of the substrates examined at 325 °C, even PTFE.

Table 1
Surface Tensions of Pitches
and Polyaromatic Model Compounds

AR-mesophase (HP Grade) at 325 °C:	27.0 mJ/m ²
A240 isotropic petroleum pitch at 150 °C:	32.5 mJ/m ²
Dimethylbenz(a)anthracene, C ₂₀ H ₁₆ , 150 °C:	26.0 mJ/m ²
Naphthalene at 127 °C[literature data]:	28.8 mJ/m ²

Table 2: Contact angles on well characterized surfaces
(all surface energies in mJ/m²)

liquid/ substrate	surface energy	disp. part	polar part	contact angle (deg)	inhibition factor F_1
for AR (HP grade) at 325 °C					
<i>on Polymers</i>					
PTFE	18	18	0	66.5	0.86
<i>on Ceramics</i>					
Borosilic. glass	67.5	33.9	33.6	26.8	0.84
Bisque alumina	78.0	33.1	44.9	40.6	0.79
Boron nitride	65.0	32.6	32.4	26.8	0.86*
Mica	60.9	31.3	29.6	26.9	0.88*
<i>on Carbons</i>					
HOPG basal	40.54	32.7	7.87	17.2	0.89*
graphite foil	42.6	33.0	9.61	23.5	0.87*
glassy carbon	42.9	33.2	9.6	13.2	0.89*
<i>on Metals</i>					
Aluminum	72.4	34.6	37.8	35.9	0.80
Iron	72.5	33.8	38.7	37.0	0.80
Silver	63.9	36.4	26.7	22.0	0.83*
Zinc	71.2	38.6	32.6	23.2	0.80
Cobalt	73.3	34.3	39.0	38.5	0.79
Platinum	78.5	34.5	44.0	39.5	0.78*
Nickel	73.2	34.8	33.4	37.3	0.79*
for Ashland A240 isotropic pitch at 150 °C					
PTFE:	18	18	0	68.0	0.92
Borosil. glass	67.5	33.9	33.6	42.1	0.85
Mica	60.9	31.3	29.6	42.2	0.89
HOPG basal	40.5	32.7	7.9	37.4	0.89
Nickel	73.2	34.8	38.4	48.6	0.80
for Dimethyl(a)anthracene, C ₂₀ H ₁₆ at 150 °C					
on PTFE:	18	18	0	55.4	0.94

* These F_1 values are approximate only, since the theory that yields F_1 is strictly valid for surfaces on which mesophase pitch exhibits "edge-on" anchoring [5]. Anchoring on the substrates marked with the asterisk is face-on (carbons, mica, silver, platinum, nickel) or unknown (boron nitride).

Theory of Equilibrium Wetting

Contact angles measured at equilibrium are amenable to thermodynamic analysis based on the surface tension of the liquid, the surface energy of the solid, and specific interactions (dispersive, polar, H-bonding, complexing) at the liquid/solid interface. An equilibrium theory for pitch wetting has been proposed [5] based on the classical Fowkes theory modified for application to pitch. The primary equation in the pitch theory is:

$$\gamma_{sl}(\phi) = \gamma_s + \gamma_l(\phi) - 2F_1(\phi) \sqrt{\gamma_s^d \gamma_l^d}(\phi) \quad (1)$$

which gives the interfacial energy, γ_{sl} , as a function of the solid surface energy, γ_s , the liquid surface tension, γ_l , and the interaction of the dispersive components of both

phases, γ_s^d , γ_l^d . The pitch is assumed to be non-polar and thus incapable of interacting with the polar component of solid surface energy [5]. Equation 1 includes a dependence of liquid and interfacial properties on the anchoring angle, ϕ , — the angle of preferred molecular orientation of pitch mesogens at the interface [5]. Finally, F_1 was proposed as an inhibition factor that describes the geometric mismatch between the solid lattice and large, planar polyaromatic molecules in pitch [5].

Equation 1 can be combined with the Young equation:

$$\gamma_s = \gamma_{sl} + \gamma_l \cos \theta \quad (2)$$

to make predictions of the contact angle, θ , by:

$$\cos \theta = -1 + 2(F_1^2 \gamma_s^d / \gamma_l^d)^{1/2} \quad (3)$$

or to yield values for the inhibition factor, F_1 from measured contact angles:

$$F_1 = (\gamma_l / 2) (1 + \cos \theta) (\gamma_s^d \gamma_l^d)^{-1/2} \quad (4)$$

The F_1 values inferred in this way are shown in Table 2. They show the expected magnitude (0.8-1) and vary over a narrow range. This agreement supports that basic assumptions of the model — that pitch interacts only with the dispersive component of the solid surface energy and that these interactions are inhibited by lattice mismatch. The equilibrium theory provides a tool for understanding how pitch will wet on a variety of substrates at equilibrium. Unfortunately, equilibrium is difficult to reach in many practical cases, especially in the case of low temperatures and complete wetting at equilibrium ($\theta_{eq} = 0$).

Theory of Non-Equilibrium Wetting: Dynamic Spreading

The equilibrium theory above gives a reasonable description of pitch wetting in the region of high fluidity (325 °C), but cannot explain the high apparent contact angles at lower temperatures, which are believed to be due to kinetic limitations on spreading. Viscous liquids other than pitch are also known to give very long equilibration times [8]. Modern theories of liquid spreading [9,10] are based on a balance of two forces: the viscous force associated with shear in the wedge-shaped leading edge of the droplet (see Fig. 3) and the unbalanced surface tension force at the contact line, $\gamma_l(\cos(\theta) - \cos(\theta_{eq}))$ where θ is the dynamic (non-equilibrium) contact angle. In the limit of complete wetting (equilibrium contact angle of zero), and where the dynamic contact angle, θ , is small, this force balance leads to:

$$dR/dt = (1/6)(\gamma_l / \mu) \theta^3 \ln(x_{max} / x_{min}) \quad (5)$$

adapted from de Gennes [9]. Here dR/dt is the spreading rate, μ the viscosity, and γ_l/μ the characteristic spreading velocity. The logarithmic term arises from integration the shear stress along the horizontal direction from $x_{max} = R$ (droplet radius) to a cutoff value, x_{min} , where a transition occurs to the precursor film. Without this cutoff, the shear rate becomes unbounded at the leading edge where the film thickness approaches zero but the fluid velocity remains finite (equal to the spreading velocity). This leads to the well-known paradox that liquid spreading could never occur at finite rates [9].

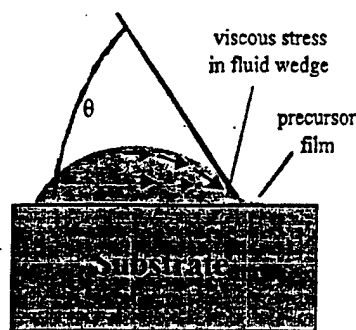


Fig. 3. Schematic of a spreading droplet. The overall shape is a spherical section from the Laplace relation when gravity is negligible (valid for small droplets). The fluid motion in the advancing wedge is analogous to that of a tank tread in the case of the no-slip condition at the substrate surface.

To predict the time dependence of the contact angle, one needs to specify droplet shape in order to relate θ to the droplet radius, R , and the known droplet volume, V_0 . In the absence of gravitational effects the drop shape is a sphere section by Laplace's law [9], for which one can derive the following exact relation:

$$V_0 = (\pi R^3 / 3 \sin \theta) [2 - 3 \cos \theta + \cos^3 \theta] \quad (6)$$

which for small θ is well approximated by $V_0 = (\pi/4) R^3 \theta$

Equations 5 and 6 were combined and used to fit the dynamic contact angle data in Fig. 2 using viscosity as a parameter. A typical transition film thickness of 10 nm was used for the logarithmic cutoff [9], and variation around this value had only small effects on the results. As seen in Fig. 2, the DeGennes theory [9] provides a good description of the dynamic pitch wetting data for viscosities of 8 Pa-s at 325 °C, 4 Pa-s at 341 °C, and 1 Pa-s at 358 °C. We could not obtain a good fit to the data at 371 °C, where the spreading time was of order 1 sec. This may be due to the violation of the assumption of creeping flow, and indeed the Reynold's number, $RV_0^{2/3}/\tau\mu$, begins to approach 1 for the short times (τ) and low viscosities (μ) in the 371 °C case.

These viscosities are similar to values reported for AR in this temperature range [3]. Exact comparisons are not possible, however, since there is no data to the authors' knowledge for the very low shear rates relevant to droplet spreading, and at least some authors report non-Newtonian flow for mesophase pitch in which the viscosity varies greatly with shear rate [3,11]. Most published studies have been conducted at shear rates from 10^3 - 10^4 sec⁻¹, while average shear rates in these droplet spreading experiments are of order 0.01-0.1 sec⁻¹.

Finally it is useful to use the dynamic theory to extrapolate spreading times to lower temperatures. White and coworkers [12] present a summary of pitch viscosity data, and quote a typical activation energy for pitch viscosity of 60 kcal/mol in the range above 8 Pa-s and 35 kcal/mol below 8 Pa-s. Using 35 kcal/mol to extrapolate from 325 °C to lower temperatures, we calculate an estimated equilibration time at 270 °C that is 20 times as long as at 325 °C, which is already much greater than 100 sec. Indeed this confirms that pitch wetting is strongly limited by spreading kinetics at 270 °C making

measurements on equilibrium contact angle in that temperature range impractical.

4. CONCLUSIONS

The wetting of solid surfaces by AR mesophase pitch depends on temperature, time, and the chemical nature of the substrate. There is strong evidence that AR wetting is limited by spreading kinetics at temperatures below 300 °C, but can approach an equilibrium state at temperature above 325 °C if sufficient time is allowed prior to measurement. Measurements of dynamic contact angle appear to follow the de Gennes theory of dynamic spreading based on the competition between surface tension driven flow and viscous dissipation. In the higher temperature range where equilibrium is approached, AR wets all substrates examined, but the contact angle varies significantly as a function of substrate. These variations are well correlated by a recent theory of equilibrium pitch wetting based on the Fowkes/Owens-Wendt theory of liquid/surface interactions modified for non-polar polyaromatics. Future work will focus on carbon fibers of various type and surface properties as wetting substrates.

ACKNOWLEDGEMENTS

Technical contributions from Chris Rulison at Kruss USA as well as the assistance of Ms. Marietta Fernandez and Lt. Scott Iacono in reducing the data are gratefully acknowledged

REFERENCES

- [1] Wapner PG, Hoffman WP, Jones S, US Patent 6,309,703, 2001.
- [2] Jian K., Shim H-S, Schwartzman A, Crawford GP, Hurt RH, *Adv. Materials* 2003; 15(2) 164-167.
- [3] Yoon, S-H, Korai Y, Mochida I, Kato I, Carbon 1994; 32(2) 273-280.
- [4] Heintz EA, Carbon 1986; 24 (2) 13-134.
- [5] Hurt RH, Krammer G, Crawford GP, Jian K, Rulison C., *Chem. of Materials* 2002; 14 4558-4565.
- [6] Owens DK, Wendt RC, *J. Appl. Polym. Sci.* 1969; 13 1741.
- [7] Padday JF, *Wetting, Spreading, and Adhesion*, Academic Press, New York, 1978.
- [8] Ogarev VA, Timonina TN, Arslanov VV, Trapeznikov AA, *J. Adhesion* 1974; 6 337-355.
- [9] de Gennes PG, *Rev. Mod. Physics*, 1985; 57(3) 827-863
- [10] Leger L, Joanny JF, *Rep. Prog. Phys.* 1992; 431-486.
- [11] Khandare PM, Zondio JW, Stansberry PB, Stille AH, Carbon 2000; 38 889-897.
- [12] White JL, Gopalokrishnan, MK, Fathollahi, B, Carbon 1994; 32(2) 301-310.